RINA'91, International Conference on Ro-Ro Safety and Vulnerability the Way Ahead, Heathrow Penta Hotel, London, 17 - 19 April 1991, Vol. I.

Reprinted: 22-03-2001
Website: www.shipmotions.nl

Report 0889-P, September 1991,
Delft University of Technology,
Ship Hydromechanics Laboratory,
Mekelweg 2, 2628 CD Delft,
The Netherlands.

Roll Motions of Ships due to Sudden Water Ingress, Calculations and Experiments

A.W. Vredeveldt (TNO) and J.M.J. Journée (DUT)

SUMMARY

Roll-on Roll-off vessels appear to be sensitive to rapid capsizing due to sudden ingress of water. Rapid capsizing is caused by a drastic decrease of static stability properties due to free surfaces, as well as by inertia effects with regard to the roll motion. In this report it is shown that the dynamic behaviour of the ship due to sudden ingress of water cannot be neglected. To this end a calculation model was developed which was verified by ingress tests. For these tests a wing tank cross-duct configuration was chosen. The results are presented in this report.

1. INTRODUCTION

The safety of ships in general has to be assessed by judging several aspects. The stability of both the intact ship and the damaged ship is of major importance. The past has shown the vulnerability of Ro/Ro vessels with regard to stability; see references [l], [2], [3] and [4].

The stability of ships is presently determined by applying quasi-static methods. Inertia effects with regard to the (roll) motions of the ship are neglected. Usually flow calculations are not carried out either, although there is one exception, which refers to the design of cross-ducts. When a cross-duct is applied a flow calculation is carried out in order to establish the minimum required cross sectional area. Such calculations usually assume a zero heel angle during the period of flooding.

The roll motion of a ship can be described by a second order differential equation where the angle of roll is used as the independent variable. On the basis of this equation, it is possible to define a natural roll period T_R. The moment of heel is determined by both the weight of water, which has flowed into the ship,

and the distance of the centre of gravity to the axis of rotation. The flow of the water into the ship can be described with a first order differential equation. From this equation a time constant T_F can be determined.

Figure 1 shows the solution of a second order differential equation with two different right hand terms. The time constants of the response and the "load" terms are indicated. From the figure, it can be seen that, when a heeling moment is applied to the ship a dynamic amplification is to be expected when this moment increases from 0 to its maximum value within the roll period T_R. When the moment increases much slower - i.e. from 0 to its maximum value during several times T_R - then a much smaller dynamic amplification can be expected.

Table 1 shows an estimate of both constants for an arbitrary chosen ferry and for a damage area with a probability of occurrence of 50 % (reference [10]).

Time constant of flow	T_F	12	[s].
Roll period	T_R	21	[s].
T_F / T_R		0.6	[-]

Table 1 Estimate of Time Constants T_F (Water Ingress Through a Damage Area) and T_R (Roll Period) for an Arbitrary Chosen Case

From this table it can be seen that the time constant related to the inflow of water may equal almost half of the roll period. Therefore a dynamic amplification is to be expected. This consideration was the main motive to carry out this project.

2. PHILOSOPHY

The aim of the work reported here was to determine whether dynamic considerations are required while judging the damage stability of ships during water ingress. In order to reach this goal a fairly straightforward approach was used. The next paragraph describes this approach.

Then on ship motions as well as on flow off fluids is fairly well developed. Therefore it is feasible to develop a calculation method which can describe both the roll motion of a ship and the flow of fluid. The method is to be verified with ingress experiments on a simple floating structure in laboratory conditions, including the effect of roll motions. Once the calculation method is verified, a systematic parameter study can be carried out on actual ships. On the basis of the parameter study, conclusions may be drawn with regard to the need to include dynamic considerations while judging damage stability. Figure 2 shows this philosophy schematically. This paper covers the first four tasks, up to and including the verification.

3. THE CALCULATION METHOD

3.1. *EQUATION OF MOTION*

Both the vertical immersion and the trim due to the water ingress are determined quasi statically, by interpolation based on the ship's hydrostatic data. No dynamics are taken into account.

The roll motion however is determined including dynamic effects. To this end the following equation of motion with

one degree of freedom is used. Coupling effects with sway and yaw motions are neglected as yet.

$$(I_{xx} + a_{44})\ddot{f} + b_{44}\dot{f} + c_{44}f = M_k$$

Equation 1

where:

I_{xx}	mass moment of inertia of the dry ship,
a_{44}	hydrodynamic mass moment of inertia due to the presence of water,
$\ddot{f}$	angular acceleration of roll angle,
b_{44}	roll damping coefficient,
$\dot{f}$	angular velocity of roll motion,
c_{44}	righting moment coefficient,
f	angle of roll,
M_k	inclining moment.

Sections 3.2, 3.3 and 3.4 give some considerations with regard to the left-hand side terms of equation (1). Section 3.5 elaborates on the heeling moment.

3.2. *SHIP'S MOMENT OF INERTIA*

The mass moment of inertia may be determined, by extending the ship's mass calculation with a radius for each mass item. Some approximate methods are available as well [5]. The hydrodynamic mass moment of inertia may be determined in several ways. Some simple estimation methods are available [8]. More elaborate methods are based on two [61 and three-dimensional potential flow methods. However the most accurate way of determining $(I_{xx} + a_{44})$ is by performing a roll decay test. The calculated rail motions as presented in Chapter 5 were based on the latter approach.

3.3. *DAMPING*

Because of viscous effects, the determination of the damping coefficient is mainly based on empirical methods [7]. Generally, only a small percentage may be determined by applying potential flow theory, whereas the larger contribution originates from viscous effects. In the calculation model the damping coefficient b_{44} is assumed to show a linear relation with the rail velocity. This assumption is acceptable since most of the damping originates from friction forces, which vary in a quadratic way with the roll velocity. Hence the following formula holds:

$$b_{44}\dot{f} = b_{44}'\dot{f}\left|\dot{f}\right|$$

Equation 2

Here again a roll decay test will yield the most reliable figures for damping. It should be noted that the dependency of the damping coefficient b_{44} on the roll velocity disturbs the linearity of the equation of motion.

3.4. *RIGHTING MOMENT*

The righting moment may be determined in a rather straightforward manner.

$$c_{44} = \frac{d}{df}\left(rg\nabla\overline{GN}_f \sin f\right)$$

Equation 3

where:

r	density of water,
g	acceleration of gravity,
∇	displaced volume of ship,
$\overline{GN}_f$	metacentric above C.o.G. of ship,
f	roll angle.

$\overline{GN}_f$ is usually available from hydrostatic calculations.

It should be noted that the righting moment coefficient c_{44} (in fact a spring "constant") depends on the roll angle, which disturbs the linearity of the equation of motion.

3.5. *HEELING MOMENT*

The heeling moment M_k may be determined by a summation of the heeling moments caused by the weight of the fluid in each compartment.

$$M_k = \sum_{i=1}^{nc} GV_i Y_i$$

Equation 4

with:

M_k	heeling moment,
r	density of water,
g	acceleration due to gravity,
v_i	volume of water in each damaged compartment i due to water ingress,
y_i	heeling lover of water volume in compartment i,
nc	number of compartments.

The volume in each compartment is calculated by applying Bernoulli's law for both the water flow and the airflow through each orifice *).
However, two adjustments are made:

1. The variation of the hydrostatic water pressure to the height of the orifice is taken into account by subdividing the orifice into horizontal strips. The flow contribution of each strip is calculated separately followed by a summation of the contributions of all strips.
2. In order to account for the pressure loss through orifices, a pressure loss coefficient is introduced.

Hence the water flow through each flow strip is determined with the next formula.

$$Q_i = \sqrt{\frac{2 \cdot \Delta P}{K \cdot r} \cdot A}$$

Equation 5

where:

Q_i	volume of water flow,
ΔP	pressure loss through strip,
K	pressure loss coefficient,
r	density of water,
A	sectional area of flow strip.

The airflow through each strip is determined with a similar formula. In order to cater for the compressibility of the air the density is not used any more.
The air pressure in each compartment can be derived from the theorem of Boyle - Gay Lussac. Thus the following formula is derived.

$$Q_1 = \sqrt{\frac{\Delta P_1 \cdot R \cdot T}{|P_1 + P_2| \cdot K} \cdot 2A}$$

Equation 6

where:

Q_1	volume of airflow,
ΔP_1	pressure loss through strip,
R	specific gas constant of air,
T	temperature of air,
P_1	pressure at "front" of strip,
P_2	pressure at "rear" of strip,
K	pressure loss coefficient,
A	flow area of flow strip.

4. MODEL TESTS

4.1. *INTRODUCTION*

As mentioned in Chapter 2, the calculation model was verified by experiments. These experiments were necessary mainly because of two reasons:

1. The calculation model needed to be verified.
2. Few data were available on pressure loss coefficients.

Since the trimming motion was expected to behave quasi statically, this motion was eliminated by using a test model which was symmetrical about the amidships. In fact this assumption requires an experimental justification as well, however this was not carried out in this project.

The dynamic behaviour of the test model had to be "ship-like" with regard to the following aspects:

1. the hydrostatic forces and moments,
2. the (hydrodynamic) mass moments of inertia and hydrodynamic damping,
3. the flow of water into the damaged compartments and
4. the flow of water between the compartments and the cross duct.

These aspects called for a fairly large test model. Moreover the sensitivity of the pressure transducers also imposed lower limits to the size of the test model. However on the other hand there were limitations to the size of the model because of the size of the test basin.

4.2. *MODEL DESCRIPTION*

Since wing tank – cross-duct configurations are used frequently; this configuration was also built into the test model. The actual dimensions of the tanks and the duct were scaled down from an existing ferry, however some deviations had to be made because of practical reasons.
Figure 3 shows the duct configuration. The hull form was chosen rectangular, because no favourable resistance characteristics are required and because of costs. The actual dimensions are dictated by the dimensions of the test basin i.e. the width of the towing tank.
Further details are shown in Table 2.

Length, L	3.000 m
Beam, B	2.100 m
Depth, D	1.250 m
Draught , T	0.625 m
Length of wing tank, l_t	1.000 m
Breadth of wing tank, b_t	0.400 m
Height of wing tank, h_t	1.250 m
Length of cross-duct, l_d	1.400 m
Breadth of cross-duct, b_d	0.200 m
Height of cross-duct, h_d	0.400 m
Height of CoG, $\overline{KG}$	0.750 m

	0.800 m
Mass of the model (displacement intact), V_i	3937.5 m^3
Moment of inertia of dry test model (dry), I_{xx} **)	1970 kgm^2

Table 2 Characteristics of the Test Pontoon

4.3 *VARIABLE AND MEASURED PARAMETERS*

Since several parameters will affect the roll motion due to sudden water ingress, it was considered to be important to carry out tests where some of these parameters were varied. Thus the results of such measurements could be used to check the results obtained by calculations. Flow calculations through cross ducts assume a stationary flow. However flow phenomena due to sudden water ingress are far from stationary. In order to obtain a preliminary idea of the error introduced by this assumption, special attention was paid to the flow of water into the test model and through the cross-duct.

The following parameters were varied:

- size of damage orifice,
- height of orifices between wing tank and duct, height of orifices in the duct,
- size of the air orifices in the top of the wing tanks,
- configuration of the cross-duct,
- height of the centre of gravity, $\overline{KG}$.

By carrying out calculations while varying the parameter values, a validation of the calculation model could be accomplished. Table 3 shows a review of the actual parameter values.

RUN. NR.	VARIATION OF:	KG	INSTRM DIAM.	HEIGHTS COMP. 1	HEIGHTS COMP. 2	HEIGHTS COMP. 3	CROSS FLOW ORIFICE HEIGHTS ZA A	ZA B	ZA C	ZA D	NR. AIRHOLES COMP 1	NR. AIRHOLES COMP 5
34	CMP. HGT.	0.747	0.400	0.275	0.275	0.275	0.225	0.225	0.225	0.225	2	2
43	DUCT ORF.	0.747	0.400	0.400	0.275	0.400	0.150	0.225	0.225	0.150	2	2
49	DUCT ORF.	0.747	0.400	0.400	0.275	0.400	0.300	0.225	0.225	0.300	2	2
51	AIR HOLE	0.747	0.400	0.400	0.275	0.400	0.225	0.225	0.225	0.225	3	3
53	pivot	0.747	0.400	0.400	0.275	0.400	0.225	0.225	0.225	0.225	2	2
55	AIR HOLE	0.747	0.400	0.400	0.275	0.400	0.225	0.225	0.225	0.225	1	1
58	AIR HOLE	0.747	0.400	0.400	0.275	0.400	0.225	0.225	0.225	0.225	0	0
59	DMG. ORF.	0.747	0.195	0.400	0.275	0.400	0.225	0.225	0.225	0.225	2	2
61	DMG. ORF.	0.747	0.239	0.400	0.275	0.400	0.225	0.225	0.225	0.225	2	2
63	DMG. ORF.	0.747	0.276	0.400	0.275	0.400	0.225	0.225	0.225	0.225	2	2
65	DMG. ORF.	0.747	0.319	0.400	0.275	0.400	0.225	0.225	0.225	0.225	2	2
120	KG	0.800	0.400	0.400	0.275	0.400	0.225	0.225	0.225	0.225	2	2

Table 3 Review of Parameter Variation (See Figure 4 as well)

Please note that the value of the intact displacement, mass moment of inertia, damping and trim ware not varied.

The following parameters were measured:

- angle of roll,
- water pressure at the bottom of each compartment,
- air pressure at the top of each compartment and
- water levels in each compartment.

The actual locations of the gauges are shown in Figure 3.

4.4 *EQUIPMENT AND TEST SET UP*

Data were recorded both in a digital way and an analogue way.

Air pressures and water pressures were measured with pressure gauges, which were in contact with the top of the tank via small tubes. Thus the gauges could remain outside the tank.

Water levels wore measured with two resistance wires per tank as is often used to measure wave heights at the bow during sea keeping experiments. Unfortunately these level gauges showed a non linear characteristic.

The angle of roll was measured with an inclinometer, which was very accurate.

Water flows and velocities were not measured. They were derived from the water the level measurements. From the level measurements, the increase of water volume in each tank could be determined. The difference between volume increases yielded the actual water flow through an orifice.

The time plots of the flow rates showed a rather erratic character. Therefore a smoothing routine was applied on the raw data of the flow rate before they could be used to derive pressure loss coefficients. Pressure data ware treated in the same way.

5. RESULTS OF MEASUREMENTS AND CALCULATIONS

Some of the input data - required to carry out the calculations - were determined experimentally.

This applies in particular to:

- mass moment of inertia $I_{xx} + a_{44}$,
- damping coefficient b_{44}',
- pressure loss coefficients K.

These properties were determined in the case where the independent variables were set as shown below:

centre of gravity above base, KG	0.747 m
area of damage orifice, A_i	0.126 m^2
cross sectional area comp. 1	0.080 m^2
cross sectional area comp. 2	0.055 m^2
cross-sectional area comp. 3	0.080 m^2
orifice area A, A_A	0.027 m^2
orifice area B, A_B	0.027 m^2
orifice area C, A_C	0.027 m^2
orifice area D, A_D	0.027 m^2
area of air hole 1, A_1	0.001 m^2
area of air hole 2, A_2	0.001 m^2

$(I_{xx} + a_{44})$ and b_{44} were determined from the results of a roll decay experiment. The pressure loss coefficients used were determined by trial and error in such a way that the calculated roll motion curve and the measured roll motion curve fitted best.

The height of the centre of gravity, $\overline{KG}$, was determined by inclining experiments. Once these properties were established they were kept constant throughout all other calculations covering other damage orifices, other cross duct dimensions and another $\overline{KG}$-value.

5.1. *ROLL MOTION*

Table 4 gives a review of some of the characteristics of the roll versus time curves.

VARIATION OF	MAX. ANGLE OF HEEL [degs] M	C	TIME REQUIRED TO REACH ZERO HEEL [sec] M	C	AREA BELOW CURVE [degs*s] M	C	RUN NR.
DUCT ORIFICE							
0.018	18.6	18.4	22.0	20.0	184	137	43
0.027	18.2	18.0	16.5	16.2	133	109	(53)
0.036	18.3	17.7	14.0	16.0	115	103	49
AIRHOLE ORIFICE							
0	17.0	15.6					58
0.000078	16.2	16.3	16.8	16.1	128	106	55
0.000157	18.2	18.0	16.5	16.2	133	109	(53)
0.000235	19.3	18.9	17.0	16.5	132	111	51
DAMAGE ORIFICE							
0.029864	10.9	12.7	21.5	20.4	127	121	59
0.059828	13.6	14.2	17.5	17.2	130	113	63
0.125663	18.2	18.0	16.5	16.2	133	109	(53)
KG							
0.747	18.2	18.0	16.5	16.2	133	109	(53)
0.8	23.0	21.0	20.5	16.8	224	133	120

Table 4 Comparison of Calculated and Measured Characteristics of Roll Versus Time (M refers to measured and C refers to calculated).

Figure 4 up to and including Figure 8 present some plots of both the calculated and the measured roll motions as a function of time. Moreover Figure 9 shows the influence of the area of the damage orifice area on the maximum roll angle.

5.2. *PRESSURE LOSS COEFFICIENTS*

From the measurements, pressure loss coefficients were determined as well. This was carried out for run 53 only where:

$\overline{KG}$:	0.750 m
D_i:	0.400 m
duct height SB:	0.275 m
duct height at CL:	0.400 m
duct height PS:	0.275 m
orifice height A:	0.225 m
orifice height B:	0.225 m
orifice height C:	0.225 m
orifice height D:	0.225 m
area airvent SB:	0.002513 m^2
area airvent PS:	0.002513 m^2

Some results are shown in Figure 10 and Figure 11.

It was found that the pressure loss coefficients depended upon the flow speed. This dependency is not mentioned in literature.

Table 5 presents both the values of the lower asymptotes of the K - flow speed curves and the values as used in the calculations.

	DAMAGE ORIFICE	ORIFICES C	D	AIR ORIFICE
Lower asymptote	3.5	0.6	1.4	
As used in calculation	1.5	2.0	2.0	

Table 5 Pressure Loss Coefficients, Values as Used in Calculations (Air Loss Coefficient from [9])

The values as used in the calculations, were determined by trial and error until in the case of run 53 the calculated maximum roll angle and the leveling time agreed with the measurement. During all other calculations these values were kept constant.

6. CONCLUSION

6.1. *MATHEMATICAL MODEL*

The mathematical description of the roll and flow phenomena seems appropriate. Figure 4 to Figure 8 show both calculated and measured roll response curves, while Table 4 gives a review.

Please note that the coefficients, as used in the calculations were determined in such a way that the roll motion of run 53 was described best. Subsequent the coefficients were kept constant.

6.2. *PRESSURE LOSS COEFFICIENTS*

Pressure loss coefficients, as measured, show a strong flow speed dependency. Current literature ([8], [9] and [10]) does not mention this dependency. Probably the dependency is due to the fact that during the tests the flow of water is far from stationary, which is a requirement for applying the concept of pressure loss coefficients. Moreover inertia effects in the fluids are neglected. The actual figures vary within a large range (0.6 - 40.0).

6.3. *OVERSHOOT*

From the measurements as well as from the calculations it can be concluded that there is a significant overshoot in the initial roll angle just after the water ingress has started. This overshoot is entirely due to inertia effects associated with the roll motion. Thus it can be stated that the dynamics of the roll motion cannot be neglected when judging the damage stability of ships. A cross duct does not seem to affect this overshoot significantly (see Table 4).

6.4. *FURTHER RESEARCH*

During discussions about this project, it was brought up that sway and yaw motions could be of significant importance. In the calculation model as reported here these motions are neglected. Some justification may be found in the reasonable agreement between calculated and measured results. However a systematic verification should be carried out.
The choice of the pressure loss coefficients is of importance for both the maximum roll angle and the time required to level out. Unfortunately the measured coefficients are not in line with literature. Moreover measurements show that these coefficients vary with flow speed, which is not reported in literature either. Therefore it is proposed to investigate this matter more extensively. It should be noted that only one of twelve measuring runs was analysed with regard to this aspect due to budget limits.

The results of the measurements and the calculations refer to a rectangular pontoon. It is essential to use the calculation method on actual ships. Once this has been done final conclusions may be drawn with regard to dynamic effects.

It seems useful to link the computer program as described here with existing programs on hydrostatic data and cross-curves. It is also useful to extend the current program with subroutines, which determine added moment of inertia and damping or establish a link with hydrodynamic programs, which can calculate such parameters.

*) *Apart from the air flow calculations, this approach is taken from the IMCO recommendations for the determination of minimum cross-duct areas [101.*

**) *Calculated with:* $I_{xx} = \frac{1}{12} V_i \left(B^2 + D^2 \right)$.

ACKNOWLEDGEMENT

The authors wish to record their appreciation of the work carried out by staff members of the Shiphydro-mechanics Laboratory of the Delft University of Technology. A special word of thanks is addressed to Mr. E. Vossnack (former head of design department of Nedlloyd Fleet Services), Mr. H. Vermeer (Netherlands Directorate General of Shipping and Maritime Affairs), Mr. D. Spanjer and Mr. J. Uwland (TNO). Finally, the authors like to thank Mr. A. van Strien (Delft University of Technology), who has been a great help with the performance of the experiments.

REFERENCES

1. Spouge, J.R., "The Technical Investigation of the Sinking of the RO/RO Ferry EUROPEAN GATEWAY", RINA Mar., No. 3, 1986.
2. Boilwood, D.T., "Ro/Ro Ship Survivability; Comments on Damage Stability Modelling", Ro/Ro-88, Gothenburg, 7-9 June 1988.
3. Braund, N.A., "Damage Stability; Research for the Future", Safe Ship/Safe Cargo Conference, London, 1978.
4. Dand, I.W., "Hydrodynamic Aspects of the Sinking of the Ferry HERALD OF FREE ENTERPRISE", The Naval Architect, May 1989.
5. Peach, et al, "The Radii of Gyration of Merchant Ships", North-East Coast of Engineers and Shipbuilding Transactions, June 1987, Page 155 - 117.
6. Journée, J.M.J., "Seaway-Delft, User Manual and Theoretical Background of Release 3.0", Ship Hydrodynamics Laboratory, Delft University of Technology, Report No. 849, January 1990.
7. lkeda Y. et al, "Prediction Method for Ship Rolling", Department of Naval Architecture, University of Osaka Prefecture, Japan, Report No. 00405, 1978.
8. Blevins R.O., "Applied Fluid Dynamics Handbook", von Nostrand Reinhold Company, New York, 1984.
9. Ireland N., "Damage Stability Model Tests", Project No. 34620, British Maritime Technology, May 1988.
10. IMCO, "Explanatory Notes to the Regulations on Subdivision and Damage Stability of Passenger Ships as Equivalent to Part B of Chapter 11 of the International Convention for Safety of life at Sea, 1960", ANNEX II, STAB XV/11.
11. Delft University of Technology, "Numerical Analysis C1", Lecture Notes (in Dutch).

NOMENCLATURE

A	flow area, m^2
a_{44}	hydrodynamic moment of inertia, kgm^2
B	beam, m
b_{44}	hydrodynamic damping coeff., Nms/rad
b_{44}'	hydrodyn. damping factor, Nms^2/rad^2
b_d	breadth of duct, m
b_t	breadth of wing tank, m
c_{44}	spring coefficient, Nm/ rad
CoG	centre of gravity
D	depth, m
ΔP	pressure loss, N/m^2
D_i	diameter of damage orifice, m
g	acceleration of gravity (9.81), m/s^2

$\overline{GN}_f$	metacentric height, m (varying with angle of heel)
h_t	height of wing tank, m
I_{xx}	ridgid moment of inertia of ship, kgm^2
K	pressure loss coefficient, N/m^2
$\overline{KG}$	height of CoG above base, m
L	length of ship, m
l_d	length of duct, m
l_t	length of tank, m
M_k	heeling moment, Nm
nc	number of compartments
$\ddot{f}$	angular roll acceleration, rad/s^2
$\dot{f}$	angular roll velocity, rad/s
f	roll angle, rad
Q	water flow, m^3/s
R	gas constant, J/(kgK)
r	density of water, kg/m^3
T	draught, m
u_i	approximative value by Euler integration
V	volume of displacement, m^3
v_{2i}	approximative value by Euler integration
v_i	approximative value by Euler integration
y_i	exact value
h_d	height of duct, m

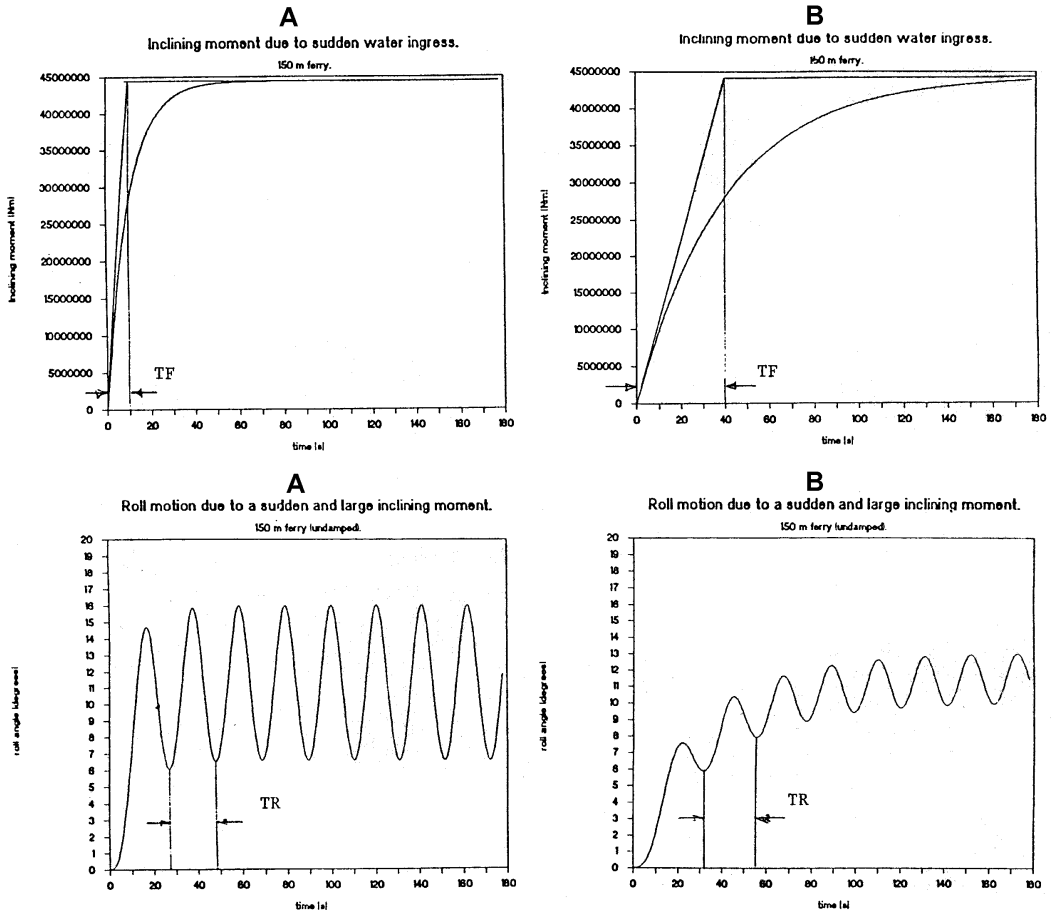

Figure 1 Rough Estimates of Roll response to Sudden Water Ingress

A: TG = 10 s, B: TF = 40 s

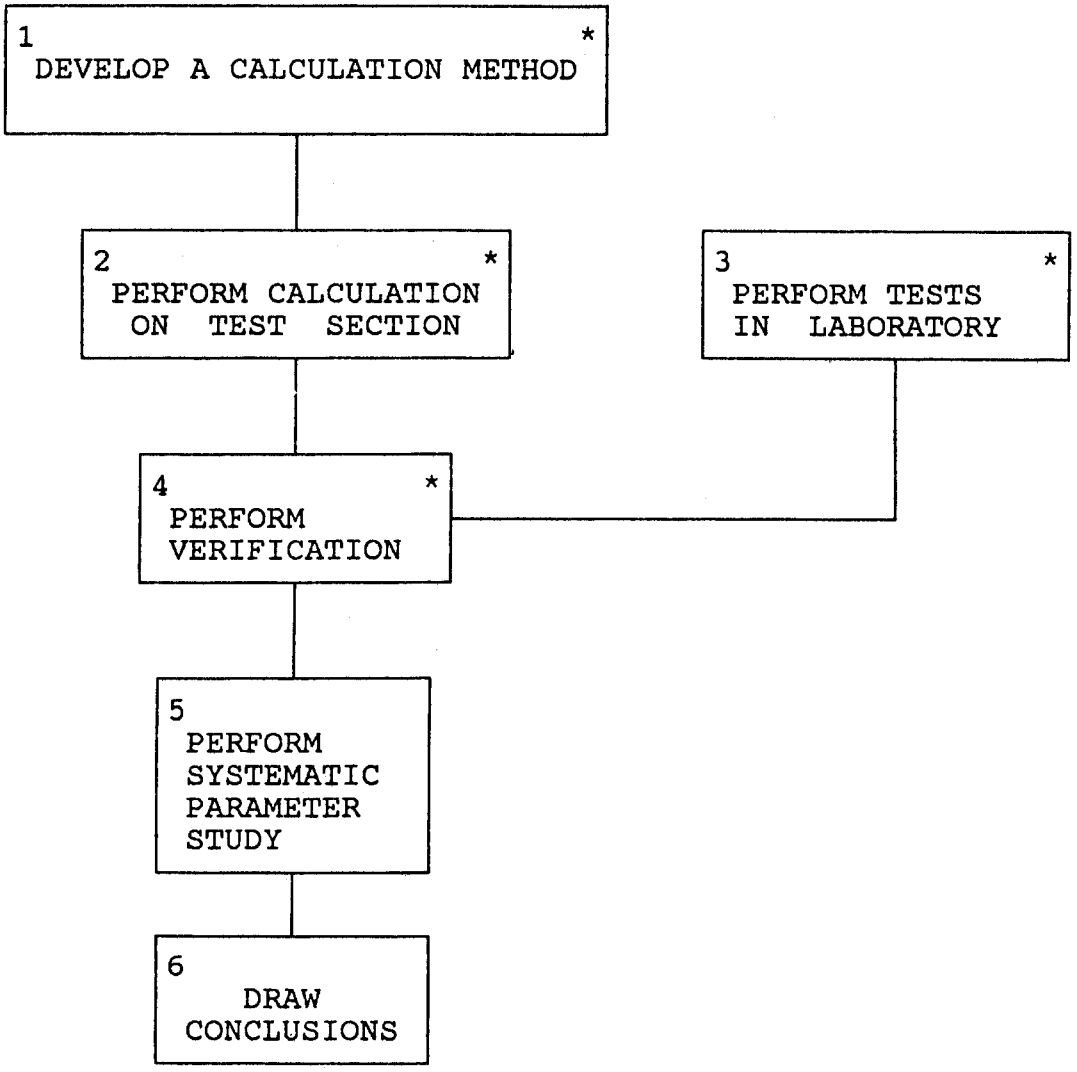

Figure 2 Schematic Representation of the Philosophy

(* indicates tasks covered in this paper)

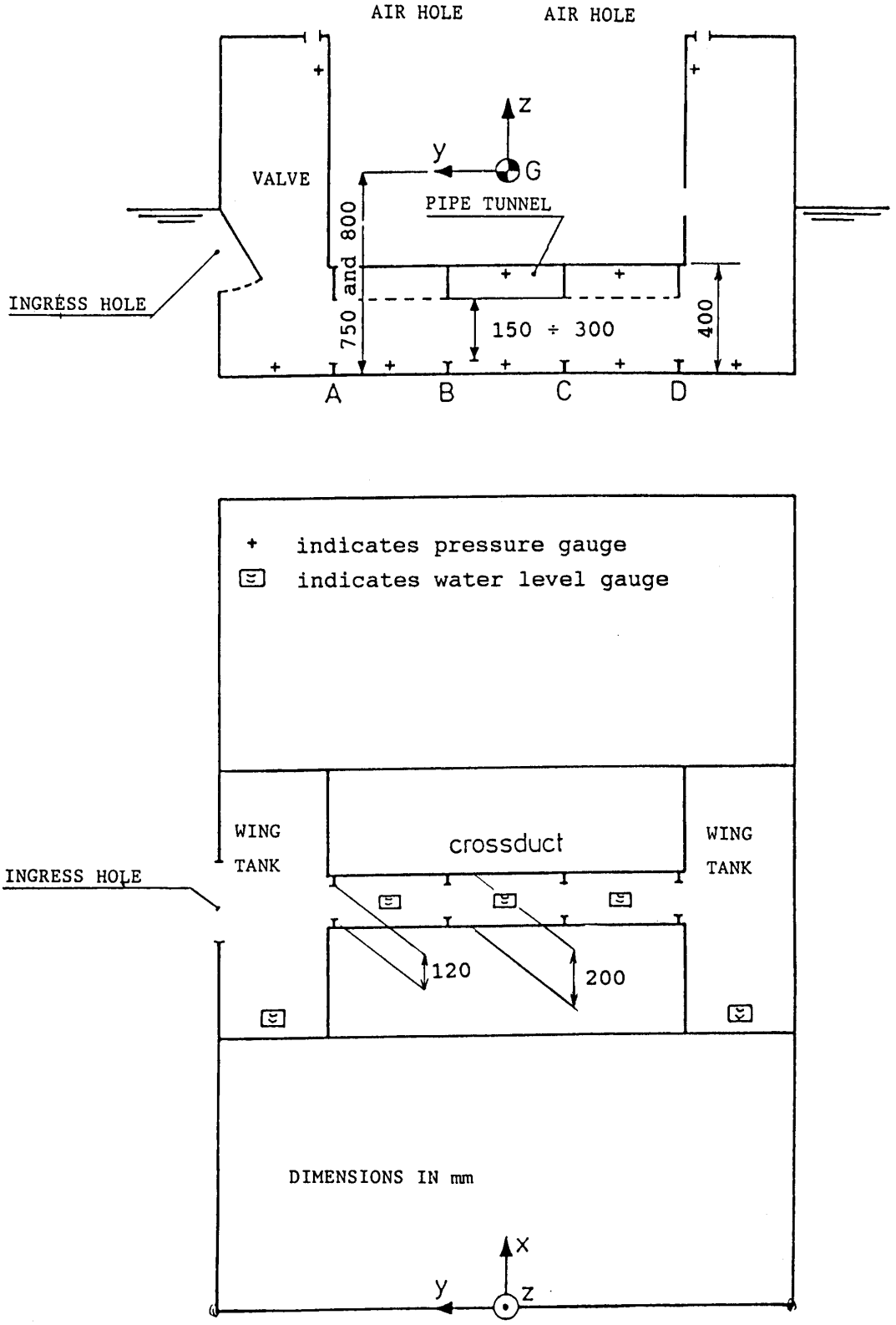

Figure 3 Cross-Section and Top View of Testmodel

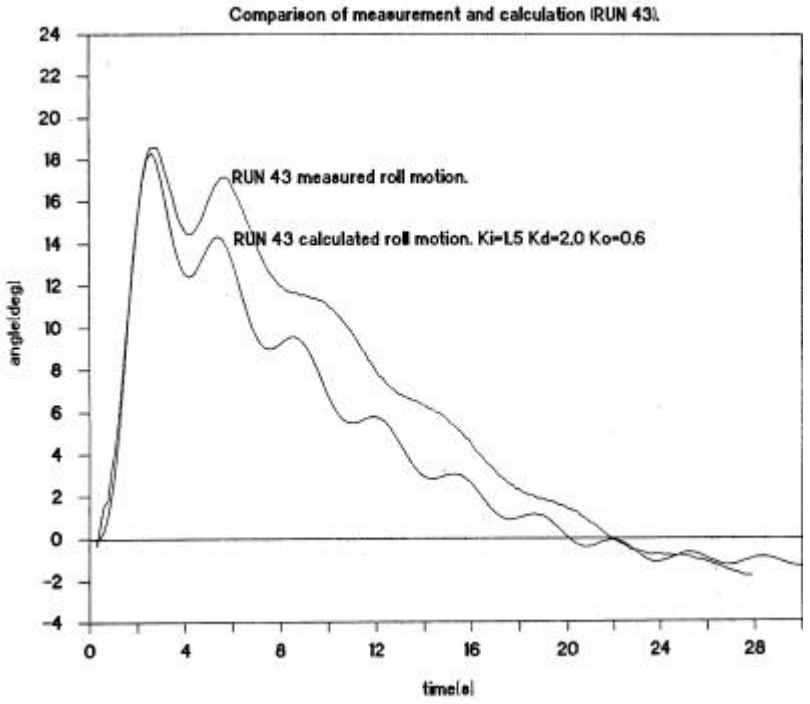

Figure 4 Roll Motion Run 43 (Decreased Duct Area)

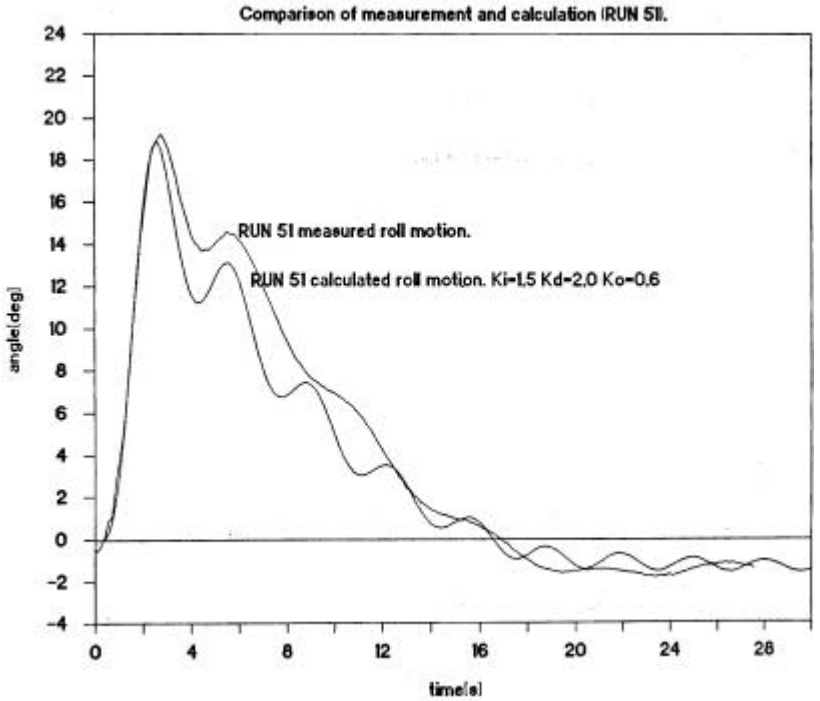

Figure 5 Roll Motion Run 51 (Area of Vent. Holes Increased)

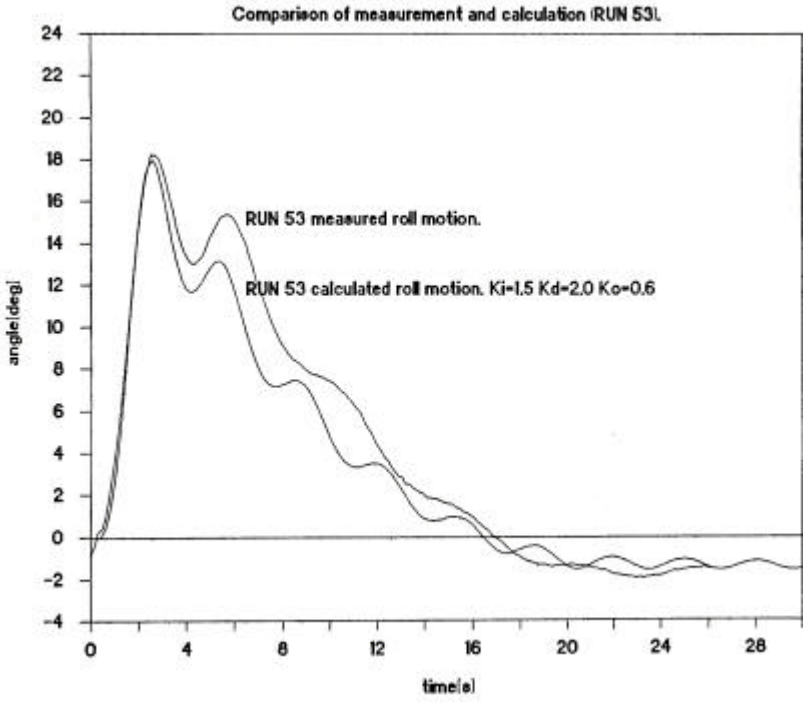

Figure 6 Roll Motion Run 53 (Initial Configuration)

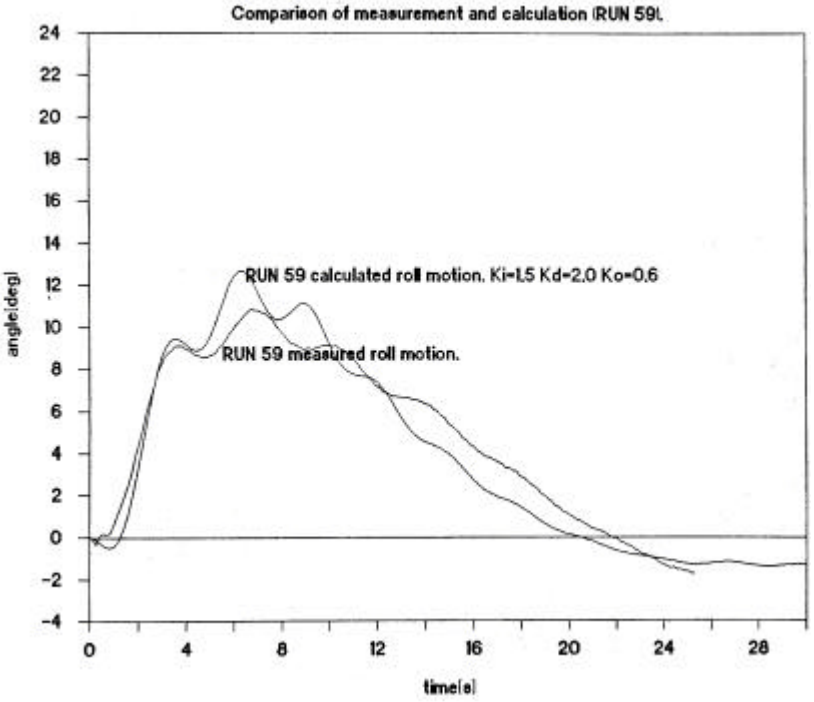

Figure 7 Roll Motion Run 59 (Damaged Orifice Decreased)

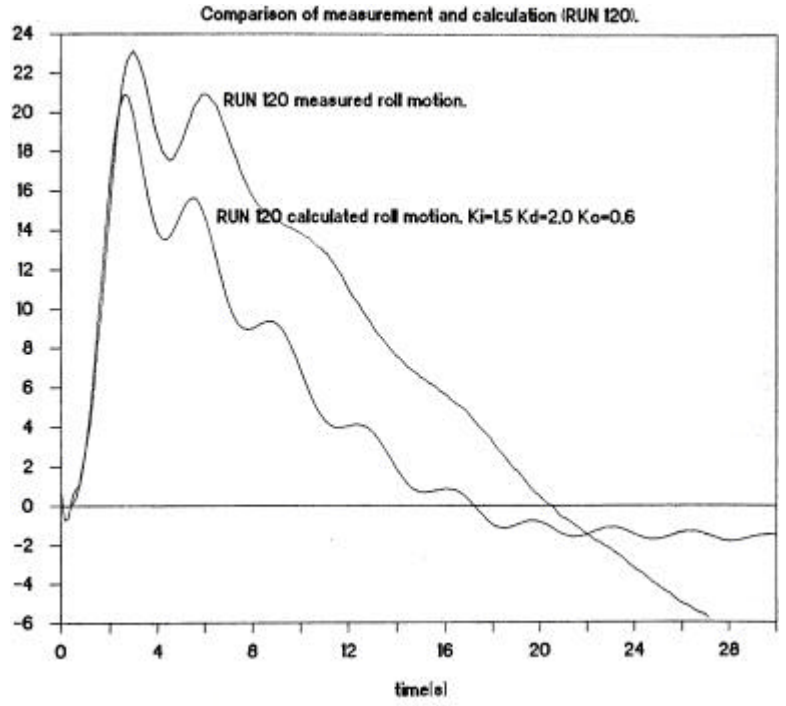

Figure 8 Roll Motion Run 120 (Height of CoG Increased)

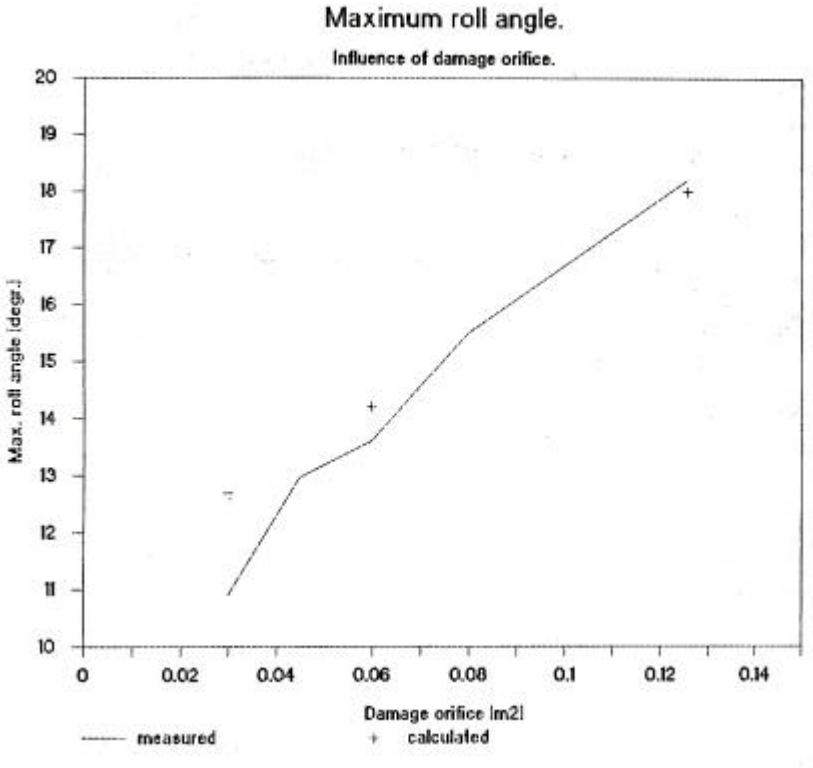

Figure 9 Maximum Roll Angle Versus Area of Damage Orifice

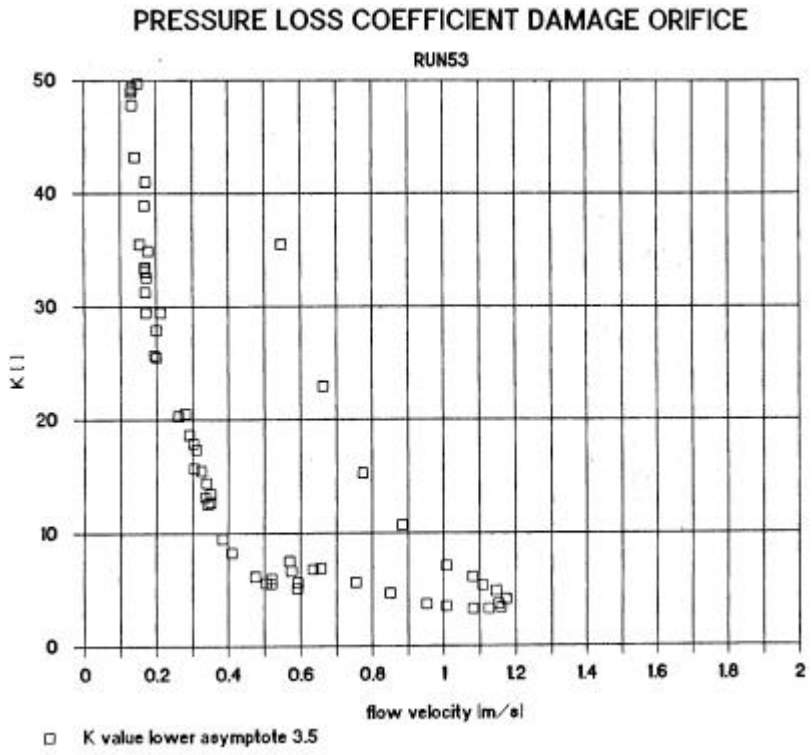

Figure 10 Pressure Loss Coefficient as Function of Flow Velocity, Damage Orifice

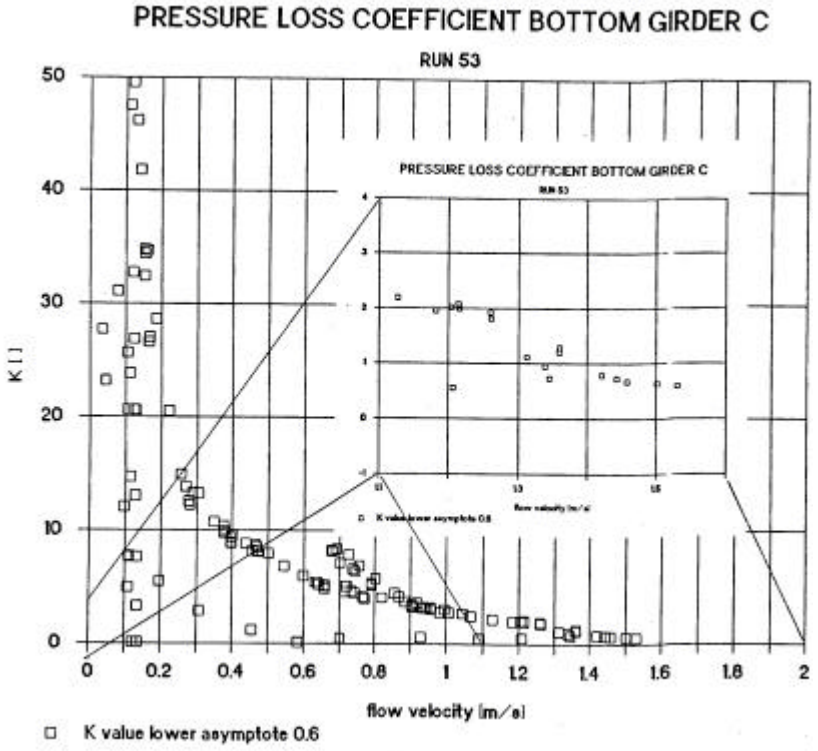

Figure 11 Pressure Loss Coefficient as Function of Flow Velocity, Orifice C (see Figure 3)